Computational electrocatalysis: methods and fundamental applications on CO2 reduction and formic acid oxidation

Granda Marulanda, L.P.

Kalemegdan
Belgrade, Serbia

1 General Introduction

"Inventions grow old and are superseded by other inventions and being the creation of the constructive schemes of mortal men, are themselves mortal. But the laws which the stars and the planets obey and have always obeyed in their paths through the heavens are unchangeable; they never grow old, and therefore they are immortal; they are part of the *eternal truth*."

M. I. Pupin (1923)[1]

Michel (Mihajlo) Idvorski Pupin refers to the laws of nature as the *eternal truth.* Perhaps, the reason why we are often in search of more accurate models to represent the operations of the world, is to come closer to its understanding, closer to this *truth*.

In the domain of computational chemistry, accuracy does not always translate to complexity. To understand the how's and why's, simple models of a target system based on the well-founded laws of quantum physics and chemistry- the laws atoms and molecules obey, can lead to scientific revelations the same way as more complex models would do, especially if the model in question is studied by a framework based on those laws. Density Functional Theory (DFT) is one of such frameworks.

In essence, the model of the target system is created by our interpretation and current understanding of the real environment. The beauty of DFT is that it can simulate this model, as if it were simulating the real world. However, sometimes the outcome from DFT does not follow exactly what we expect from chemical concepts or from what we see experimentally. There are two major reasons for this discrepancy. One is that the model is not encapsulating the important interactions, or "something" is not being considered, and this could be because we do not have enough information or knowledge of the real system. The second reason is the limitation of DFT itself, more precisely the overestimations or underestimations of system properties; mostly a fault of the approximate functionals used in DFT. Knowing these limitations is immensely important, as it allows us to discriminate the results, and also encourages us to improve the methods and consequently propose hypotheses to build new knowledge.

In this thesis, we investigate simple computational electrochemical methods, their usability and ways to improve their accuracy (***Chapters 2-4***), and apply them to the study of Formic acid oxidation and production via a collaborative experimental and computational study (***Chapter 5-6)***

1.1 Theoretical Background

It took several decades for quantum-chemical methods to develop into what we have today, all driven by the same ultimate goal: to be able to compute the values of physical properties that describe chemical systems, for instance, energy, bond lengths, bond frequencies, and how such properties change as the system interacts with different environments. In heterogeneous (electro)catalysis, we are interested in the interaction between solids (the electrode), molecules (the reactants or intermediates), and the electrolyte (solvent and ions).

This section gives a summary of the theoretical background behind Quantum Chemistry and DFT gathered from various books and articles.[2–6] In quantum mechanics, particles are described by the wave function, ψ. This function of state contains all the information about their physical properties. Besides, $|\psi|^2$ is the probability density of finding the particle in a certain region of space, and the value of a physical property is obtained through the action of a corresponding Hermitian operator on the wave function. Here, we focus on the stationary (time-independent) Schrödinger equation (1926).[7]

$$\hat{H}\psi(r_i) = E\psi(r_i) \tag{1.1}$$

Eq.1.1 describes a one-particle system i, with coordinates r_i. $\hat{H}$ is the Hamiltonian operator, the energy operator, defined as; $\hat{H} = \hat{T} + \hat{V}$, the sum of the kinetic energy operator, $\hat{T}$, and the potential energy operator $\hat{V}$. For atoms, the low weight of the electrons compared to the heavy nuclei allows treating the dynamics of electrons and nuclei separately. This allows approximating the full (time dependent) Schrödinger equation by an electronic Schrödinger equation, that is stationary and does not contain the kinetic energy of the ions, and a nuclear Schrödinger equation, that can often be treated classically.

This is the so-called Born-Oppenheimer approximation (B-O, 1927).[8] Within this approximation the electronic Hamiltonian operator is

$$\hat{H} = \hat{T}_e + \hat{V}_{ee} + \hat{V}_{en} + \hat{V}_{ext} \tag{1.2}$$

and it takes into account the kinetic energy of the electrons and their potential energy (arising from electron-electron interactions, $\hat{V}_{ee}$, attractive electron-nucleus interaction, $\hat{V}_{en}$, and an external potential, $\hat{V}_{ext}$). The electron-nucleus interaction is then treated as the attraction between the electron and the field of the fixed nucleus. In Eq.1.1 the eigenfunction ψ corresponding to the lowest energy eigenstate E is the ground state wave function. E is then the corresponding ground state energy of the electronic one-electron wave function at 0K.

However, we are primarily interested in finding the ground-state energy of interacting solids and molecules, that is a system of many atoms, meaning a system of many electrons, and so the ground state of such system can be determined if we solve the following equation, known as the many-electron Schrödinger equation.

$$\hat{H}\psi(r_1, r_{2,} r_3 \dots r_N) = E\psi(r_1, r_{2,} r_3 \dots r_N) \quad 1.3$$

This equation "is the starting point for computational materials science, and the ground-state properties of any system can be determined by solving this equation, if we have a method to solve it."

J. G. Lee[6]

Eq.1.3 depends on 3x N coordinates as the number of N particles increases and, therefore, it becomes too complex to solve, both analytically and numerically, when there are electrons interacting with all the other electrons at the same time. This is where Density Functional Theory (DFT) proposes a simplification that allows the computation of an approximate solution to Eq.1.3.

Before discussing the quantum mechanical framework of Density Functional Theory, we note that other quantum chemical-mechanical frameworks have been developed to solve the many-body Schrödinger equation. One of the mathematical problems is the presence of correlation, that is the electrons interacting with the field created by the other electrons. The Hartree-Fock (HF) method (1930) gives an approximation to this interaction, and although it gives reasonable results for small molecules, it does not do so well for solids. The error in the approximation, arises from replacing the exact electron-electron interaction with a mean-field interaction. Besides the HF method, other methods worth mentioning for solving the many-body Schrödinger equation are: variational methods such as the configuration interaction method (CI), non-variational methods such as the couple cluster method (CC), many-body perturbation Theory (MBPT) and Møller-Plesset approaches.

1.1.1 Density Functional Theory (DFT)

The bases of Density Functional Theory rely on the Hohenberg-Kohn theorems[9] and the equations derived by Kohn and Sham.[10] The first theorem states that the ground-state electronic density, $\rho_0(r)$, contains the same precise information about the system as the ground-state wave function ψ_0 and, therefore, the ground-state wave function can be expressed as a functional of the ground-state electronic density. This allows to write the ground-state expectation value of the Hamiltonian as a functional of ρ_0. Knowing the molecular Hamiltonian, the many-electron Schrödinger equation can be solved and the ground-state energy of the system and numerous electronic properties of the system can be obtained. Thus, in practice, the first theorem establishes that the ground-state energy of a many-body system, $E_0[\rho]$, is a functional of the ground-state electronic density, which depends on an external potential, $\nu_{ext}(r)$, The total energy functional, $E_v[\rho]$, can be represented as

$$\mathrm{E_\nu}[\rho] = \mathrm{F}[\rho] + \int \nu_{ext}(r)\rho(r)\mathrm{d}r \qquad 1.4$$

where $\mathrm{F}[\rho] = \mathrm{T}[\rho] + V_{ee}[\rho]$, is a universal functional of the density and contains the kinetic energy, $\mathrm{T}[\rho]$, and the electron-electron interaction, $V_{ee}[\rho]$, and is independent of $\nu_{ext}(r)$.

The second theorem (proven with the variational principle[4]) states that there exists an energy functional, $E_\nu[\rho]$, that is minimized by the correct or ideal ground-state electron density, ρ_0, in the external potential, $\nu_{ext}(r)$, and that the minimal value of the energy functional represents the ground-state energy of the system, E_0.

$$E_\nu[\rho] \geq E_\nu[\rho_0] = E_0 \qquad 1.5$$

The theorems provide the fundamental principles of DFT but do not allow for its practical use. The practical use of DFT lies within the Kohn-Sham formalism.[10] In this formalism, the Schrödinger equation is written for a fictitious system of non-interacting particles moving in an effective potential with the same density as a system of interacting particles. The following is a one-electron Schrödinger-like equation, named the Kohn-Sham equation, and can be solved iteratively.

$$\left(-\frac{1}{2}\nabla^2 + \nu_0\right)\phi_i = \varepsilon_i\phi_i \qquad 1.6$$

The eigenvalue ε_i is the Kohn-Sham energy of the Kohn-Sham orbital ϕ_i, ν_0 is the effective potential, and the electronic density distribution is calculated by summing all the occupied Kohn-Sham orbitals, ϕ_i .

$$\rho(r) = \sum_i^N |\phi_i(r)|^2 \qquad 1.7$$

The general expression of the total energy of the ground state in this formalism is

$$\mathrm{E}[\rho] = \nu_{ext}(r) + \mathrm{T}[\rho] + \nu_{Coulomb}(\rho) + E_{xc}[\rho] \qquad 1.8$$

The first term on the right-hand side is the external potential, the second term is the kinetic energy of the non-interacting electrons (the fictitious Kohn-Sham system), the third term represents the Coulomb repulsion of the electrons, and the fourth term is the exchange and correlation energy, which includes all interactions not accounted for by the other terms (see below). The exchange and correlation energy, $E_{xc}[\rho]$, is the only term in the Kohn-Sham formalism that cannot be computed from first principles. To assess the energy of the real system it is necessary to approximate this unknown term.

Therefore, the usefulness of DFT depends on the ability to find approximations to the exchange and correlation energy functional in a way that they can represent the system of interest in an accurate and time-effective manner.[11]

The exchange-correlation energy is the sum of the exchange energy, E_x, and the correlation energy, E_c, Eq.1.9.

$$E_{xc} = E_x + E_c \tag{1.9}$$

The exchange energy results from the anti-symmetry of the electronic wave function, takes into account the repulsive interaction between electrons of the same spin (Pauli exclusion principle), and can be evaluated exactly. The correlation energy results from the tendency of electrons to stay away from each other to decrease the Coulombic interaction. It is more pronounced for electrons of opposite spins as they are more likely to occupy the same orbitals. Exact electronic correlation cannot be calculated analytically. Besides the quantum exchange and correlation effects, the term, E_{xc}, contains the correction to the fictitious non-interacting system's kinetic energy from the real system's kinetic energy (ΔT = real -non-real).

Nowadays, various approximations exist for the exchange-correlation energy functional, $E_{XC}[\rho]$. Here are some of them:

- Local density approximation (LDA)[10]
  - Commonly used for the description of bulk metals and surfaces, its geometric predictions are usually accurate. However, it has difficulties when describing molecules and ionic systems where the electron density changes rapidly in space. It tends to overestimate binding energies and fails to reproduce ionization potentials.
- Generalized gradient approximation functionals, (GGAs)
  - Give good results for molecular geometries and ground-state energies. The most commonly used are: PW91,[12] PBE,[13] RPBE[14].
- Hybrid functionals,
  - These are a linear combination of the (exact) exchange calculated with HF and exchange-correlation energies from other approximations. They are widely used for molecules and solids with localized electrons. Common hybrid functionals are PBE0 (25% of exact exchange combined with PBE exchange-correlation),[15,16] HSE,[17] B3LYP[18] and the Minnesota meta-hybrids.[19]

DFT can be applied to many different systems, to name a few: solids, gases, liquids, polymers, ice, and chemical solutions. Depending on the system that we want to study, specific basis sets are required. The basis set is a group of functions that expand the Kohn-Sham orbitals, ϕ_i, and their linear combination describes the wave function of the system. The basis set can be local (atom-centered orbitals), non-local (expanded through space) and augmented. Local basis sets are preferable to represent atoms and molecules with orbitals localized around the atoms. A commonly used local basis set is the Gaussian basis set. John Pople, who shared the Noble Prize with Walter Kohn in 1998, named the computational chemistry code "Gaussian" after these orbitals. Due to their local nature, they cannot describe well long-range interactions. Augmented basis sets include additional basis functions to those already present on the atoms, basically adding additional "subshells". Non-local basis sets are based on plane-wave functions, which require the use of periodic-boundary conditions, and are the gold standard for solids.

1.1.2 Free energies and adsorption potentials

The first and main motivation of this thesis is to outline simple computational methods based on first principles calculations using DFT for electrochemical systems. I will focus on affordable methods that can provide a tradeoff between computational expense and accuracy. Specifically focus on solvation effects near the surface of the electrode, the use of thermodynamic cycles to compute solution-phase energies of charged species, and the description of a correction scheme to detect gas-phase errors on the free energies of target molecules important for calculating adsorption processes in electrocatalysis. The second motivation of this thesis is to apply these simple methods to study complex adsorption processes at the $Pd_{ML}Pt(111)$ electrode surface. All the adsorption processes investigated experimentally were performed by Dr. Xiaoting Chen from our group.

Now we zoom out from the quantum chemistry regime and move our focus toward the thermodynamics of the system, which is obtained from the mathematical manipulation of the energies obtained from the DFT calculations. Often, the questions we try to answer do not require intensive computational resources: affordable and accurate simplifications are enough. In the context of electrocatalysis, we are interested in energies of adsorption of species at the interface between the catalyst and the electrolyte. The thermodynamic property that can provide such information is the Gibbs free energy of the reaction, $G(T,P) = U + PV - TS$, where, T and P are the temperature and pressure, U is the internal energy, P and V are pressure and volume and, in general, we are interested in processes at standard conditions, namely, 1 atm and 298.15 K.

To calculate the free energies of adsorption processes, we require the energies of the individual components of the system. As shown in Figure 1.1, we need the energy of the species in the gas phase, the energies of the solution-phase species (those in the bulk of the solution), the energies of the interacting electrode-adsorbate system, and finally the energy of the electrode itself.

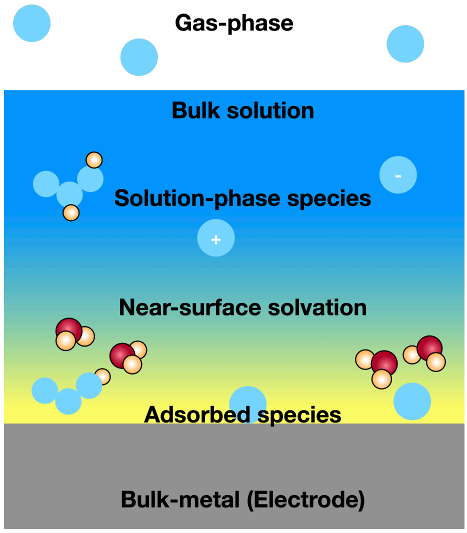

FIGURE 1.1
Illustration of the electrochemical environment and the different levels of abstraction as analyzed with DFT.

The reaction free energies are calculated as the difference of the individual free energies of the reactants and products of the chemical reaction we are investigating.

$$\Delta G^\circ = \sum G_{products} - \sum G_{reactants} \qquad 1.10$$

The individual free energies are calculated as,

$$G^\circ = E_{DFT} + E_{ZPE} + \int_{T=0}^{T} C_p \, dT - TS \qquad 1.11$$

E_{DFT} is the relative energy given by the DFT simulation extrapolated to 0 K, E_{ZPE} is the zero-point vibrational energy calculated using statistical mechanics equations within the harmonic oscillator approximation, as shown in Eq.1.12,[20] where h is Planck's constant ($4.135667662 \times 10^{-15} eV \cdot s$) and ν_i are the frequencies of the vibrational modes i, in energy terms expressed as ε_i. T is the temperature (298.15 K) and S is the entropy. For adsorbates, S contains only the vibrational contributions calculated using Eq.1.13,[20] and for gas-phase species, S includes all entropy contributions and is taken from standard thermodynamic tables.[21] In Eq. 1.13, k_B is the Boltzmann constant, 3N is the number of modes per atom of the adsorbate, $\beta = 1/k_B T$, and ε_i are the energies obtained from the calculated frequencies. The free energy of the surface slab is approximated as the energy without the contributions from the zero-point energy and entropy.[22]

$$E_{ZPE} = \sum_{i=1}^{n} \frac{1}{2} h\nu_i \qquad 1.12$$

$$S_{vib} = k_B \sum_{i}^{3N} \left[-ln\left(1 - e^{\beta\varepsilon_i}\right) + \frac{\beta\varepsilon_i}{e^{(\beta\varepsilon_i - 1)}} \right] \qquad 1.13$$

Note that within this thesis the enthalpic correction term ($\int_{T=0}^{T} C_p \, dT$) in Eq. 1.11, determined from heat capacity data, is neglected unless stated otherwise. When computing reaction energies, this term can often be neglected for systems with no hindered rotations without much loss of accuracy.

For an adsorption reaction like Eq.1.14, $* \mathrm{n}H_2O$ represents the surface with adsorbed water, $\mathrm{A_{(g)}}$ is a gas-phase molecule, $H^+ + e^-$ are a solvated proton and an electron, and $* [\mathrm{AH - nH_2O}]$ is the co-adsorbed hydrogenated molecule and water system. In ***Chapter 4***, we will discuss in detail how to determine the errors associated to the formation energies of gas-phase species and why it is useful to correct them.

$$* nH_2O + A_{(g)} + H^+ + e^- \rightarrow * [AH - nH_2O] \qquad 1.14$$

Within the computational hydrogen electrode approach,[23] the energy corresponding to the proton-electron pair is set equal to $\frac{1}{2}\mu_{H_2} - \mathrm{neU}$, where U is the electrode potential in the reversible hydrogen electrode (RHE) scale, so that the free energy of adsorption of Eq.1.14 is:

$$\Delta G_{ads}^{*[AH-nH_2O]} = G_{*[AH-nH_2O]} - G_{*nH_2O} - G_{A\,(g)} - \frac{1}{2}\mu_{H_2} + neU \qquad 1.15$$

Using free energies also allows to express the results in terms of potentials[24] using the Nernst equation for a reduction reaction:

$$\Delta G^\circ = -\mathrm{nF}U_{eq}^\circ \qquad 1.16$$

n is the number of moles of electrons transferred in the reaction, F is the Faraday constant (96.485 kJ $\mathrm{mol^{-1}}$ $\mathrm{V^{-1}}$ $\mathrm{eq^{-1}}$) and U_{eq}° is the standard equilibrium potential of the cell, referred to the NHE.

For an adsorption process, we can determine the standard equilibrium potential U_{ads}° of reaction 1.16 when the free energy of adsorption in Eq.1.15 is set equal to zero, $\Delta G_{ads} = 0$.

$$U^{\circ}_{ads} = \frac{G_{*[AH-nH_2O]} - G_{*nH_2O} - G_{A\,(g)} - G_{H^+}}{-n|e|} \quad 1.17$$

The adsorption energy can be linearly shifted through the value of U, the last term of Eq.1.15.

Thanks to the computational hydrogen electrode (CHE) model[23], we can calculate the energetics of various electrochemical processes with DFT involving a fixed number of proton-electron pairs. The CHE is widespread in the computational electrochemistry community. Other simplifications used to model the electrochemical system are the treatment of the solution-phase environment through the incorporation of a solvation model; implicit solvation, [25–35] explicit[36–43] solvation or explicit near-surface solvation, also known as micro-solvation. [44–46] In the work presented in this PhD thesis, solvation effects are applied through the explicit near-surface solvation model.

Another simple model, which will be discussed in more detail in ***Chapter 3***, is the use of tabulated equilibrium standard redox potentials and simple thermodynamic cycles to determine the free energy of a charged species in bulk solution. This allows for the calculation of equilibrium potentials for reactions in which there is not an equal number of proton and electrons. Although this model is not new, we discuss its usefulness and implications in detail.

1.2 Applications – Electrochemical formic acid oxidation and CO_2 reduction reactions

The second motivation of this thesis is to applied the DFT methods discussed in the first part to study fundamental questions pertaining to formic acid oxidation and production on the $Pd_{ML}Pt(111)$ electrode surface. More specifically, we aim to understand the adsorption processes on the bare $Pd_{ML}Pt(111)$ and elucidate the poisoning mechanisms during the oxidation and reduction reactions.

1.2.1 Practical Motivation

One of the quests of major focus toward a sustainable society is that of increasing the usage of renewables as a source of energy and decreasing the usage of fossil fuels. The latter increase greenhouse gas emissions (CH_4, CO_2, N_2O and natural gas), correlated to the increase of global temperature, leading to negative consequences such as global warming and climate change. CO_2 is responsible for more than half of the total emissions.[47]

Renewable energy can be harvested from wind turbines, solar panels, etc. At the moment, we still rely on petroleum and natural gas as our primary source of energy, as shown in Figure 1.2. In principle, we can produce renewable energy and store that energy in chemical bonds with electrochemical cells. In electrolysers, renewable electricity can convert water and CO_2 into fuels such as hydrogen, methanol and formic acid. In fuel cells, hydrogen, methanol, or formic acid, are converted back into electrical energy through spontaneous electrochemical reactions at the two electrodes. Figure 1.3 illustrates a direct formic acid fuel cell (DFAFC). The corresponding half-cell reactions at the anode and the cathode appear in Table 1.1.

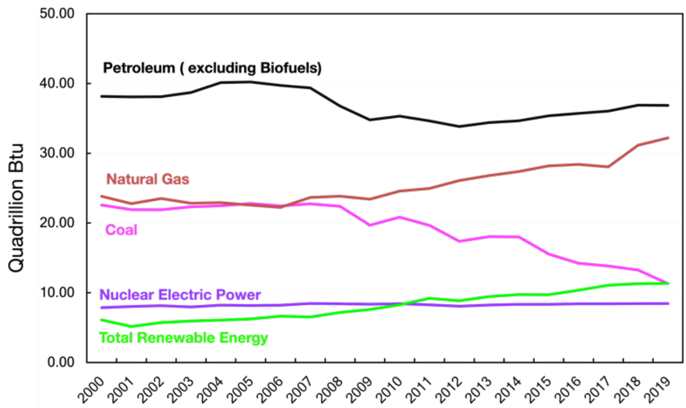

FIGURE 1.2
Energy consumption from different sources between the years 2000-2019. Data source: The U.S Energy Information Administration as per the International Energy Outlook of 2019.[48]

A fuel cell can offer high energy conversion efficiency and its operation is clean, as long as the fuels are produced from renewable electricity (contrary to combustion processes using fossil resources). Fuel cells contain an ion-conducting electrolyte or membrane, a fuel inlet, an oxidant inlet (oxygen source), an outlet for the reaction products, and two electrodes (anode and cathode). What makes fuel cells lose efficiency in general are the overvoltages required to drive the reactions at the anode and the cathode at a given current density. The further these overvoltages are from the equilibrium potentials of the corresponding half reactions, the less efficient the cell is.

The electrodes in a fuel cell are either the catalyst itself or contain the catalysts dispersed as nanoparticles on a conductive support. The catalyst should be able to enhance the kinetics of the reaction (high activity), and it should also be selective and stable. That is why many research efforts have been devoted to develop catalysts for fuel cells for both anode and cathode, but most importantly for the latter where the sluggish oxygen reduction reaction takes place.

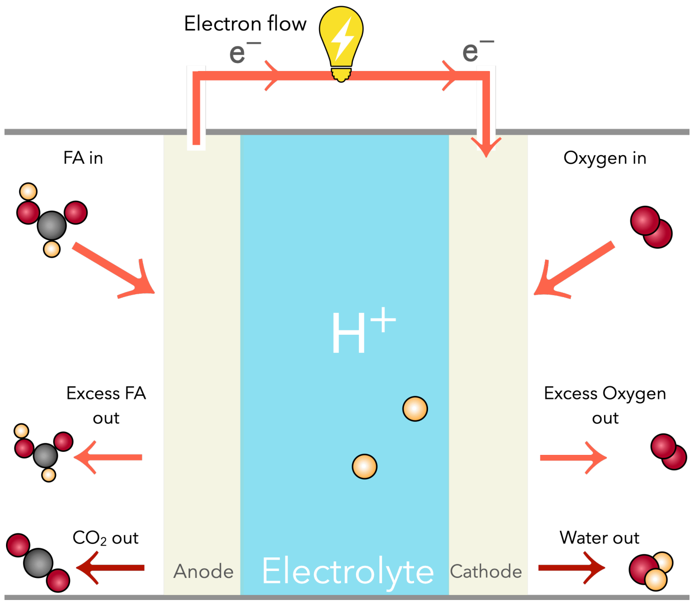

FIGURE 1.3
Illustration of a simplified direct formic acid fuel cell (DFAFC). Hydrogen: light yellow, Oxygen: red, Carbon: dark grey. The fuel, formic acid (FA), is fed to the cell to reach the anode where the oxidation reaction occurs producing CO_2, protons, and electrons. The electrons flow from the anode to the cathode through an external circuit and the protons pass through the ion conducting-electrolyte to the cathode where they combine with oxygen and electrons to produce water. The fuel and oxidant that do not react, exit the cell as excess reactants.

Figure 1.3 illustrates a (DFAFC).[49–51] In this cell, formic acid (FA) is the fuel. Since FA, is liquid at room temperature and contains two hydrogen atoms, it is also referred to as "liquid hydrogen" and "hydrogen-carrier".[52,53] The half-cell anodic (oxidation of formic acid (FA)) and cathodic (oxygen reduction), reactions are shown in Table 1.1. The overall reaction is

$$HCOOH(l) + \frac{1}{2}O_2(g) \rightarrow CO_2(g) + H_2O(l) \qquad 1.18$$

and its cell potential is, $U_{cell} = (1.23 - (-0.11)\ V\ vs\ SHE)$[54] $= 1.34\ V\ vs\ SHE$.
DFAFCs have attracted commercial attention because FA can be stored at standard atmospheric pressures, increasing its appeal in the portable market with respect to hydrogen, which requires high pressure tanks to be stored. Furthermore, the performance with perfluoro sulfonic acid membranes like Nafion® is better than methanol,[55,56] Alongside the commercial attention, the electrocatalytic oxidation of FA attracts fundamental attention because FA is a simple model molecule to understand the oxidation reaction of other more complex organic molecules.[57]

Scalability and commercialization of DFAFCs at the moment is stagnant due to the deactivation of their commercial Pt-based electrocatalysts. The deactivation is due to poising of the electrocatalysts with CO. Research efforts have been focused on finding alternative catalysts that can tolerate CO poisoning during the oxidation. Pd-based catalysts have shown to be a good alternative, primary because Pd poisons at a slower rate than Pt. However, Pd is still not an ideal catalyst for large-scale production of DFAFCs, due to their poor stability. Alternatives combining Pt- or Pd-based catalysts with other metals have shown improvements, not only on the stability but also toward CO poisoning.[58–66] However, the fundamental explanation on why various materials seem to improve their CO tolerance remains elusive, and, therefore, proposes an interesting research question warranting further investigation. In ***Chapter 6*** we aim to provide insight into this question by studying $Pd_{ML}Pt(111)$, a bimetallic catalyst, made of the two pure metals with the highest activity towards formic acid oxidation. It is also important to note that PdPt catalysts are highly active for the CO_2 reduction reaction. They can achieve CO_2 reduction to HCOOH at low overpotentials, and CO poisoning tolerance during the reduction rection is observed, as well.[67] Thus, they are appealing as bifunctional electrocatalysts for CO_2 reduction and FA oxidation.

Table 1.1 enumerates different types of fuel cells at different operating temperatures and the corresponding reactions at the anode and the cathode. Each of the half-cell reactions can be catalyzed by different materials that have been developed and optimized for the specific reactions.

TABLE 1.1

Fuel cells currently in use and in development, data obtained and adapted from reference[68] except when specified otherwise.

	Operating Temp. (°C)	Anode	Cathode
AFC (Alkaline)	<100	$H_2 + 2OH^- \rightarrow 2H_2O + 2e^-$	$\frac{1}{2}O_2 + H_2O + 2e^- \rightarrow 2OH^-$
PEM (Polymer Electrolyte Membrane)	60-120	$H_2 \rightarrow 2H^+ + 2e^-$	$\frac{1}{2}O_2 + 2H^+ + 2e^- \rightarrow H_2O$
DMFC (Direct Methanol)	60-120	$CH_3OH + 2H_2O \rightarrow CO_2 + 6H^+ + 6e^-$	$\frac{3}{2}O_2 + H_2O + 2e^- \rightarrow 2OH^-$
DFAFC (Direct Formic Acid)	50-80[69]	$HCOOH \rightarrow CO_2 + 2H^+ + 2e^-$	$\frac{1}{2}O_2 + 2H^+ + 2e^- \rightarrow H_2O$
PAFC (Phosphoric Acid)	160-220	$H_2 \rightarrow 2H^+ + 2e^-$	$\frac{1}{2}O_2 + 2H^+ + 2e^- \rightarrow H_2O$
MCF (Molten Carbonate)	600-800	$H_2 + CO_3^{2-} \rightarrow H_2O + CO_22 + 2e^-$	$\frac{1}{2}O_2 + CO_2 + 2e^- \rightarrow CO_3^{2-}$
SOFC (Solid Oxide)	800-1000	$H_2 + O^{2-} \rightarrow H_2O + 2e^-$	$\frac{1}{2}O_2 + 2e^- \rightarrow O^-$

1.2.2 Scientific Motivation

The fundamental motivation of the second part of this research comes from the need to know why PdPt catalysts show tolerance toward CO poisoning compared to Pt, during both oxidation of formic acid and reduction of CO_2 to formic acid.

To this end, we use well-defined surfaces of Pd and Pt in this research because the atomic-level control they provide can deliver a fundamental understanding of the underlying mechanisms we are interested in, specifically, the tolerance of $Pd_{ML}Pt(111)$ toward CO. Furthermore, there is a vast literature on the topic, particularly on Pt(111), that we can use to shape our understanding of the research questions that motivate us. Also, results obtained on single-crystal surfaces are ideally suitable for comparison to DFT calculations.

The formic acid oxidation reaction involves the transfer of two protons and electrons to form CO_2, as shown below.

$$\mathrm{HCOOH} \rightleftarrows \mathrm{CO_2(g)} + 2\,\mathrm{H^+} + 2\mathrm{e^-} \qquad 1.19$$

The first mechanism for formic acid oxidation on Pt was proposed by Capon and Parsons,[70] involving parallel catalytic routes called the direct and indirect pathways. They proposed that formic acid oxidizes to an active intermediate, *COOH, that could either undergo a dehydration (indirect pathway), where a poisoning species seems to form, or a dehydrogenation (direct pathway). In the indirect pathway, the poisoning species, now known as *CO,[71,72] can be further oxidized to CO_2, while in the direct pathway the intermediate is directly oxidized to CO_2. Later, Cuesta and coworkers[73] using attenuated total reflectance-surface-enhanced infrared absorption spectroscopy (ATR-SEIRAS), suggested that the active intermediate for both the indirect and direct paths is adsorbed formate.

The proposal of formate as the active intermediate became controversial when evidence suggested that the faradaic current during the oxidation reaction was observed to increase faster than the formate coverage did,[72] and also because in this configuration, both oxygens are bound to the surface, and breaking the C-H bond would cost about 1.0 eV.[74] Therefore, Chen and coworkers[72] proposed that formate is more a spectator than an active intermediate. Using DFT, Janik[74] and Schwarz[26] proposed that the active intermediate for the direct pathway could be formate with C-H down, as in this configuration the breakage of the C-H bond has a low or no barrier at all.

We can transfer this knowledge to other active catalysts such as Pd. Palladium is highly active for the formic acid oxidation reaction, and for some years CO poisoning was not visible in experiments. Vielstich showed in 1988[75] that the catalyst could be deactivated by strongly adsorbed species, but evidence of the identity of the species was elusive. Nowadays, we have evidence that the deactivation of the catalysts is caused by CO formation on palladium, although at a much slower rate than on Pt.[76] In addition, in relevant conditions for fuel cells, the catalyst is deactivated only after long periods of operation.[77] Therefore, palladium is still an attractive catalyst because it is more tolerant to CO poisoning than Pt during formic acid oxidation. One of the drawbacks, however, is its difficult preparation and cleaning, especially for single-crystal electrodes, limiting it to fundamental research.

As a result, research on bimetallic catalysts containing Pd and another easy to prepare and clean metal such as Pt, is a promising alternative to understand CO tolerance and increase the catalyst stability. Palladium overlayers grown epitaxially on Pt(hkl) have been investigated by various research groups, namely, those of Kolb,[78,79] Feliu,[80,81] Markovic[82,83] and our group in Leiden.[84] These catalysts showed high activity toward formic acid oxidation and clear resistance toward poisoning during the oxidation.[78] Furthermore, Kortlever and coworkers[85] showed the quasi-reversible behavior of the bimetallic catalyst for both formic acid oxidation and carbon dioxide reduction, as expected for a two-electron transfer reaction.[86] This research was followed by work by Chen et al.[87] on single crystal catalysts of Pd overlayers on Pt(100), i.e. $Pd_{ML}Pt(100)$, to obtain a more fundamental understanding of the reaction mechanisms.

In the second part of this PhD thesis, we will expand the previous research and focus on comparative studies supported by DFT and experiments performed by Dr. Chen from our group on well-defined surfaces of Pt(111) and $Pd_{ML}Pt(111)$. First, we study in detail the adsorption processes on the bare surface and then we move on to the catalytic reactions, namely, formic acid oxidation and carbon dioxide reduction, with a focus on understanding the absence of CO poisoning observed with the $Pd_{ML}Pt(111)$ catalysts.

1.3 Scope and outline of this PhD thesis

This PhD thesis is organized in two parts: the first part, ***Chapters 2-4***, discusses DFT methodologies based on affordable and simple approximations to facilitate the usability of DFT for electrochemical systems, aspiring toward precise, robust and practical procedures. It specifically focuses on near-surface solvation and methods to calculate accurate reference free energies of charged species and gas-phase species. In the second part, ***Chapters 5*** and ***6***, these methods are applied to the study of electrocatalytic adsorption processes on $Pd_{ML}Pt(111)$ and its CO tolerance during the formic acid oxidation reaction and carbon dioxide reduction. The simulations are complemented by relevant experimental results, performed by Dr. Xiaoting Chen[84] from the experimental counterpart of the CASC research group.

In ***Chapter 2***, we do a survey of the influence of different functionals, specifically those including and not including long-range interactions, on the near-surface solvation of hydroxide on different Pt near-surface alloys Pt-M-Pt (111). The calculated hydroxide solvation energies allow us to divide the functionals into two groups: over-binding and under-binding functionals. We observe that extrapolating solvation energies is safe when done within the same group of functionals. The difference on average between the solvation energies in these two groups is 0.15 eV. For accurate catalyst design for the oxygen reduction reaction, it is then recommended not to extrapolate energies from one group to the other, as the criteria for catalyst design for this reaction is $\Delta G_{OH} - \Delta G_{OH}^{Pt(111)} \approx 0.1 - 0.15$ eV.

In ***Chapter 3***, we review and discuss a method to obtain free energies of charged species in bulk solution, important for electrochemical adsorption processes. This method uses simple electrochemical thermodynamic cycles to map the energy of a neutral species with that of a charged species using a tabulated half-cell equilibrium reduction potential that contains the charged and the neutral species. With this method we can avoid DFT calculations of the charged species in bulk solution, which is challenging to perform with DFT. The method can be used to calculate equilibrium adsorption potentials involving charged species.

Chapter 4 presents a systematic workflow used to determine errors associated to organic functional groups on 27 different gas-phase molecules. We use this method for CO_2 reduction and CO reduction reactions and show that it is easy to implement and inexpensive, providing a very good match with experimental onset potentials determined for the CO_2 reduction reaction to CO. This method can be used to pinpoint errors of other molecules not studied here and increase the accuracy of DFT results for different exchange correlation functionals.

Chapter 5 discusses a comparative study of the adsorption processes on the well-defined $Pd_{ML}Pt(111)$ and Pt(111) by means of DFT calculations and experiments using cyclic voltammetry. The adsorption of hydroxide, hydrogen, oxygen and water was investigated at different coverages and as a function of applied potential, from which we built surface phase diagrams. We also studied the adsorption of various anions and found that they interact more strongly on $Pd_{ML}Pt(111)$ compared to Pt(111). Our results showed that the "hydrogen" region in the CV of $Pd_{ML}Pt(111)$ can be more accurately described as a "hydrogen-hydroxyl-cation-anion" region.

Chapter 6 extends the investigation from ***Chapter 5*** to the electro-oxidation of formic acid to carbon dioxide, and the reverse reaction, that is the electroreduction of carbon dioxide to formic acid. We show the role of formate during the oxidation reaction as a spectator, the coverage of which prevents *CO poisoning at $Pd_{ML}Pt(111)$ at oxidizing potentials. During the electroreduction, $Pd_{ML}Pt(111)$ is poisoned by *CO at higher negative potentials compared to Pt(111). We show that the activation of the poisoning path is related to the adsorption of *COOH at earlier potentials on Pt than on $Pd_{ML}Pt(111)$.

1.4 References

(1) Pupin, M. (Mihajlo). *From Immigrant to Inventor*; Charles Scribner's Sons: New York, London, 1923.

(2) Capelle, K. A Bird's-Eye View of Density-Functional Theory. *arXiv:cond-mat/0211443v5* **2006**.

(3) Ferro-Costas, D.; Pendás, Á. M.; González, L.; Mosquera, R. A. Beyond the Molecular Orbital Conception of Electronically Excited States through the Quantum Theory of Atoms in Molecules. *Phys. Chem. Chem. Phys.* **2014**, *16* (20), 9249–9258.

(4) *Ideas of Quantum Chemistry*; Piela, L., Ed.; Elsevier: Amsterdam, 2007.

(5) Bader, R. F. W. *Atoms in Molecules: A Quantum Theory*; Clarendon Press: Oxford, 1994.

(6) Lee, J. G. *Computational Materials Science: An Introduction*; CRC Press, 2011.

(7) Schrödinger, E. Quantisierung Als Eigenwertproblem. *Ann. Phys.* **1926**, *385* (13), 437–490.

(8) Born, M.; Oppenheimer, R. Zur Quantentheorie Der Molekeln. *Ann. Phys.* **1927**, *389*, 457–484.

(9) Hohenberg, P.; Kohn, W. Inhomogeneous Electron Gas. *Phys. Rev.* **1964**, *136* (3B), B864–B871.

(10) Kohn, W.; Sham, L. J. Self-Consistent Equations Including Exchange and Correlation Effects. *Phys. Rev.* **1965**, *140* (4A), A1133–A1138.

(11) Kohn, W. Nobel Lecture: Electronic Structure of Matter---Wave Functions and Density Functionals. *Rev. Mod. Phys.* **1999**, *71* (5), 1253–1266.

(12) Perdew, J. P.; Burke, K.; Wang, Y. Generalized Gradient Approximation for the Exchange-Correlation Hole of a Many-Electron System. *Phys. Rev. B* **1996**, *54* (23), 16533–16539.

(13) Perdew, J. P.; Burke, K.; Ernzerhof, M. Generalized Gradient Approximation Made Simple. *Phys. Rev. Lett.* **1996**, *77* (18), 3865–3868.

(14) Hammer, B.; Hansen, L. B.; Nørskov, J. K. Improved Adsorption Energetics within Density-Functional Theory Using Revised Perdew-Burke-Ernzerhof Functionals. *Phys. Rev. B* **1999**, *59* (11), 7413–7421.

(15) Perdew, J. P.; Ernzerhof, M.; Burke, K. Rationale for Mixing Exact Exchange with Density Functional Approximations. *J. Chem. Phys.* **1996**, *105* (22), 9982–9985.

(16) Adamo, C.; Barone, V. Toward Reliable Density Functional Methods without Adjustable Parameters: The PBE0 Model. *J. Chem. Phys.* **1999**, *110* (13), 6158–6170.

(17) Heyd, J.; Scuseria, G. E.; Ernzerhof, M. Hybrid Functionals Based on a Screened Coulomb Potential. *J. Chem. Phys.* **2003**, *118* (18), 8207–8215.

(18) Stephens, P. J.; Devlin, F. J.; Chabalowski, C. F.; Frisch, M. J. Ab Initio Calculation of Vibrational Absorption and Circular Dichroism Spectra Using Density Functional Force Fields. *J. Phys. Chem.* **1994**, *98* (45), 11623–11627.

(19) Zhao, Y.; Truhlar, D. G. The M06 Suite of Density Functionals for Main Group Thermochemistry, Thermochemical Kinetics, Noncovalent Interactions, Excited States, and Transition Elements: Two New Functionals and Systematic Testing of Four M06-Class Functionals and 12 Other Functionals. *Theor Chem Account* **2008**, *120* (1), 215–241.

(20) Fultz, B. Vibrational Thermodynamics of Materials. *Prog. Mater. Sci.* **2010**, *55*, 247–352.

(21) Chase, Jr., M. W.; Davies, C. A.; Downey, Jr., J. R.; Frurip, D. J.; MacDonald, R. A.; Syverud, A. N. NIST-JANAF Thermochemical Tables. *J. Phys. Chem. Ref. Data* **1985**, *Suppl. 1 to Vol. 14*, 1856.

(22) Atkins, P. W. *Atkins' Physical Chemistry*, 7th ed.; Paula, J. de, Series Ed.; Physical chemistry; Oxford [etc.] : Oxford University Press, 2002.

(23) Nørskov, J. K.; Rossmeisl, J.; Logadottir, A.; Lindqvist, L.; Kitchin, J. R.; Bligaard, T.; Jónsson, H. Origin of the Overpotential for Oxygen Reduction at a Fuel-Cell Cathode. *J. Phys. Chem. B* **2004**, *108* (46), 17886–17892.

(24) Inzelt, G. Crossing the Bridge between Thermodynamics and Electrochemistry. From the Potential of the Cell Reaction to the Electrode Potential. *ChemTexts* **2014**, *1* (1), 2.

(25) Letchworth-Weaver, K.; Arias, T. A. Joint Density Functional Theory of the Electrode-Electrolyte Interface: Application to Fixed Electrode Potentials, Interfacial Capacitances, and Potentials of Zero Charge. *Phys. Rev. B* **2012**, *86* (7), 075140.

(26) Schwarz, K. A.; Sundararaman, R.; Moffat, T. P.; Allison, T. C. Formic Acid Oxidation on Platinum: A Simple Mechanistic Study. *Phys. Chem. Chem. Phys.* **2015**, *17* (32), 20805–20813.

(27) Sundararaman, R.; Schwarz, K. Evaluating Continuum Solvation Models for the Electrode-Electrolyte Interface: Challenges and Strategies for Improvement. *The Journal of Chemical Physics* **2017**, *146* (8), 084111.

(28) Mathew, K.; Sundararaman, R.; Letchworth-Weaver, K.; Arias, T. A.; Hennig, R. G. Implicit Solvation Model for Density-Functional Study of Nanocrystal Surfaces and Reaction Pathways. *J. Chem. Phys.* **2014**, *140* (8), 084106.

(29) Mathew, K.; Hennig, R. G. Implicit Self-Consistent Description of Electrolyte in Plane-Wave Density-Functional Theory. *arXiv:1601.03346 [cond-mat]* **2016**.

(30) Ludwig, T.; Gauthier, J. A.; Brown, K. S.; Ringe, S.; Nørskov, J. K.; Chan, K. Solvent–Adsorbate Interactions and Adsorbate-Specific Solvent Structure in Carbon Dioxide Reduction on a Stepped Cu Surface. *J. Phys. Chem. C* **2019**, *123* (10), 5999–6009.

(31) Garcia-Ratés, M.; López, N. Multigrid-Based Methodology for Implicit Solvation Models in Periodic DFT. *J. Chem. Theory Comput.* **2016**, *12* (3), 1331–1341.

(32) Dupont, C.; Andreussi, O.; Marzari, N. Self-Consistent Continuum Solvation (SCCS): The Case of Charged Systems. *J. Chem. Phys.* **2013**, *139* (21), 214110.

(33) Nishihara, S.; Otani, M. Hybrid Solvation Models for Bulk, Interface, and Membrane: Reference Interaction Site Methods Coupled with Density Functional Theory. *Phys. Rev. B* **2017**, *96* (11), 115429.

(34) Melander, M. M.; Kuisma, M. J.; Christensen, T. E. K.; Honkala, K. Grand-Canonical Approach to Density Functional Theory of Electrocatalytic Systems: Thermodynamics of Solid-Liquid Interfaces at Constant Ion and Electrode Potentials. *J. Chem. Phys.* **2018**, *150* (4), 041706.
(35) Sundararaman, R.; Letchworth-Weaver, K.; Schwarz, K. A. Improving Accuracy of Electrochemical Capacitance and Solvation Energetics in First-Principles Calculations. *J. Chem. Phys.* **2018**, *148* (14), 144105.
(36) Filhol, J.-S.; Neurock, M. Elucidation of the Electrochemical Activation of Water over Pd by First Principles. *Angew. Chem. Int. Ed.* **2006**, *45* (3), 402–406.
(37) McCrum, I. T.; Janik, M. J. PH and Alkali Cation Effects on the Pt Cyclic Voltammogram Explained Using Density Functional Theory. *J. Phys. Chem. C* **2016**, *120* (1), 457–471.
(38) Kolb, M. J.; Wermink, J.; Calle-Vallejo, F.; Juurlink, L. B. F.; Koper, M. T. M. Initial Stages of Water Solvation of Stepped Platinum Surfaces. *Phys. Chem. Chem. Phys.* **2016**, *18* (5), 3416–3422.
(39) Morais, R. F. de; Kerber, T.; Calle-Vallejo, F.; Sautet, P.; Loffreda, D. Capturing Solvation Effects at a Liquid/Nanoparticle Interface by Ab Initio Molecular Dynamics: Pt201 Immersed in Water. *Small* **2016**, *12* (38), 5312–5319.
(40) Liu, S.; White, M. G.; Liu, P. Mechanism of Oxygen Reduction Reaction on Pt(111) in Alkaline Solution: Importance of Chemisorbed Water on Surface. *J. Phys. Chem. C* **2016**, *120* (28), 15288–15298.
(41) Karlberg, G. S. Adsorption Trends for Water, Hydroxyl, Oxygen, and Hydrogen on Transition-Metal and Platinum-Skin Surfaces. *Phys. Rev. B* **2006**, *74* (15), 153414.
(42) Tripkovic, V.; Skúlason, E.; Siahrostami, S.; K. Nørskov, J.; Rossmeisl, J. The Oxygen Reduction Reaction Mechanism on Pt(111) from Density Functional Theory Calculations. *Electrochim. Acta* **2010**, *55*,(27), 7975–7981.
(43) Gauthier, J. A.; Dickens, C. F.; Chen, L. D.; Doyle, A. D.; Nørskov, J. K. Solvation Effects for Oxygen Evolution Reaction Catalysis on IrO2(110). *J. Phys. Chem. C* **2017**, *121* (21), 11455–11463.
(44) Mills, J. N.; McCrum, I. T.; Janik, M. J. Alkali Cation Specific Adsorption onto Fcc(111) Transition Metal Electrodes. *Phys. Chem. Chem. Phys.* **2014**, *16* (27), 13699–13707.
(45) Calle-Vallejo, F.; F. de Morais, R.; Illas, F.; Loffreda, D.; Sautet, P. Affordable Estimation of Solvation Contributions to the Adsorption Energies of Oxygenates on Metal Nanoparticles. *J. Phys. Chem. C* **2019**, *123* (9), 5578–5582.
(46) Rendón-Calle, A.; Builes, S.; Calle-Vallejo, F. Substantial Improvement of Electrocatalytic Predictions by Systematic Assessment of Solvent Effects on Adsorption Energies. *Appl. Catal. B* **2020**, *276*, 119147.
(47) US EPA, O. Inventory of U.S. Greenhouse Gas Emissions and Sinks https://www.epa.gov/ghgemissions/inventory-us-greenhouse-gas-emissions-and-sinks (accessed Mar 23, 2021).
(48) Capuano, D. L. International Energy Outlook 2020 (IEO2020). **2019**, 7.
(49) Yu, X.; Pickup, P. G. Recent Advances in Direct Formic Acid Fuel Cells (DFAFC). *J. Power Sources* **2008**, *182* (1), 124–132.

(50) Fang, Z.; Chen, W. Recent Advances in Formic Acid Electro-Oxidation: From the Fundamental Mechanism to Electrocatalysts. *Nanoscale Adv.* **2021**, *3* (1), 94–105.
(51) Aslam, N. M.; Masdar, M. S.; Kamarudin, S. K.; Daud, W. R. W. Overview on Direct Formic Acid Fuel Cells (DFAFCs) as an Energy Sources. *APCBEE Procedia* **2012**, *3*, 33–39.
(52) Eppinger, J.; Huang, K.-W. Formic Acid as a Hydrogen Energy Carrier. *ACS Energy Lett.* **2017**, *2* (1), 188–195.
(53) Grasemann, M.; Laurenczy, G. Formic Acid as a Hydrogen Source – Recent Developments and Future Trends. *Energy Environ. Sci.* **2012**, *5* (8), 8171–8181.
(54) Bratsch, S. G. Standard Electrode Potentials and Temperature Coefficients in Water at 298.15 K. *J. Phys. Chem. Ref. Data* **1989**, *18* (1), 1–21.
(55) Rhee, Y.-W.; Ha, S. Y.; Masel, R. I. Crossover of Formic Acid through Nafion® Membranes. *Journal of Power Sources* **2003**, *117* (1), 35–38.
(56) Kim, H. S.; Morgan, R. D.; Gurau, B.; Masel, R. I. A Miniature Direct Formic Acid Fuel Cell Battery. *Journal of Power Sources* **2009**, *188* (1), 118–121.
(57) Boronat-González, A.; Herrero, E.; Feliu, J. M. Heterogeneous Electrocatalysis of Formic Acid Oxidation on Platinum Single Crystal Electrodes. *Current Opinion in Electrochemistry* **2017**, *4* (1), 26–31.
(58) Jiang, K.; Zhang, H.-X.; Zou, S.; Cai, W.-B. Electrocatalysis of Formic Acid on Palladium and Platinum Surfaces: From Fundamental Mechanisms to Fuel Cell Applications. *Phys. Chem. Chem. Phys.* **2014**, *16* (38), 20360–20376.
(59) Kang, Y. S.; Choi, D.; Cho, J.; Park, H.-Y.; Lee, K.-S.; Ahn, M.; Jang, I.; Park, T.; Ham, H. C.; Yoo, S. J. Highly Active and Durable Ordered Intermetallic PdFe Electrocatalyst for Formic Acid Electrooxidation Reaction. *ACS Appl. Energy Mater.* **2020**, *3* (5), 4226–4237.
(60) Brandt, K.; Steinhausen, M.; Wandelt, K. Catalytic and Electro-Catalytic Oxidation of Formic Acid on the Pure and Cu-Modified Pd(111)-Surface. *J. Electroanal. Chem.* **2008**, *616* (1), 27–37.
(61) Ji, Y.; Zhao, R.; Zhang, G.; Chen, Y.; Tang, Y.; Lu, T. Room-Temperature Synthesis and Electrocatalysis of Carbon Nanotubes Supported Palladium–Iron Alloy Nanoparticles. *Electrochimica Acta* **2013**, *111*, 898–902.
(62) Gojković, S. Lj.; Tripković, A. V.; Stevanović, R. M.; Krstajić, N. V. High Activity of Pt4Mo Alloy for the Electrochemical Oxidation of Formic Acid. *Langmuir* **2007**, *23* (25), 12760–12764.
(63) Kang, Y.; Qi, L.; Li, M.; Diaz, R. E.; Su, D.; Adzic, R. R.; Stach, E.; Li, J.; Murray, C. B. Highly Active Pt3Pb and Core–Shell Pt3Pb–Pt Electrocatalysts for Formic Acid Oxidation. *ACS Nano* **2012**, *6* (3), 2818–2825.
(64) Casado-Rivera, E.; Volpe, D. J.; Alden, L.; Lind, C.; Downie, C.; Vázquez-Alvarez, T.; Angelo, A. C. D.; DiSalvo, F. J.; Abruña, H. D. Electrocatalytic Activity of Ordered Intermetallic Phases for Fuel Cell Applications. *J. Am. Chem. Soc.* **2004**, *126* (12), 4043–4049.
(65) Xu, D.; Bliznakov, S.; Liu, Z.; Fang, J.; Dimitrov, N. Composition-Dependent Electrocatalytic Activity of Pt-Cu Nanocube Catalysts for Formic Acid Oxidation. *Angew. Chem. Int. Ed.* **2010**, *49* (7), 1282–1285.

(66) Hwang, E.; Kim, H.; Park, H.; Lim, T.; Kim, Y.-T.; Ahn, S. H.; Kim, S.-K. Pd–Sn Alloy Electrocatalysts for Interconversion Between Carbon Dioxide and Formate/Formic Acid. *J. Nanosci. Nanotechnol* **2017**, *17* (10), 7547–7555.
(67) Kortlever, R.; Peters, I.; Koper, S.; Koper, M. T. M. Electrochemical CO2 Reduction to Formic Acid at Low Overpotential and with High Faradaic Efficiency on Carbon-Supported Bimetallic Pd–Pt Nanoparticles. *ACS Catal.* **2015**, *5* (7), 3916–3923.
(68) Carrette, L.; Friedrich, K. A.; Stimming, U. Fuel Cells – Fundamentals and Applications. *Fuel Cells* **2001**, *1* (1), 5–39.
(69) Rees, N. V.; Compton, R. G. Sustainable Energy: A Review of Formic Acid Electrochemical Fuel Cells. *J Solid State Electrochem* **2011**, *15* (10), 2095–2100.
(70) Capon, A.; Parsons, R. The Oxidation of Formic Acid on Noble Metal Electrodes: II. A Comparison of the Behaviour of Pure Electrodes. *J. Electroanal. Chem. Interf. Electrochem.* **1973**, *44* (2), 239–254.
(71) Beden, B.; Bewick, A.; Lamy, C. A Study by Electrochemically Modulated Infrared Reflectance Spectroscopy of the Electrosorption of Formic Acid at a Platinum Electrode. *J. Electroanal. Chem. Interf. Electrochem.* **1983**, *148* (1), 147–160.
(72) Chen, Y.-X.; Heinen, M.; Jusys, Z.; Behm, R. J. Bridge-Bonded Formate: Active Intermediate or Spectator Species in Formic Acid Oxidation on a Pt Film Electrode? *Langmuir* **2006**, *22* (25), 10399–10408.
(73) Cuesta, A.; Cabello, G.; Gutiérrez, C.; Osawa, M. Adsorbed Formate: The Key Intermediate in the Oxidation of Formic Acid on Platinum Electrodes. *Phys. Chem. Chem. Phys.* **2011**, *13* (45), 20091–20095.
(74) Neurock, M.; Janik, M.; Wieckowski, A. A First Principles Comparison of the Mechanism and Site Requirements for the Electrocatalytic Oxidation of Methanol and Formic Acid over Pt. *Faraday Discuss.* **2008**, *140* (0), 363–378.
(75) Solis, V.; Iwasita, T.; Pavese, A.; Vielstich, W. Investigation of Formic Acid Oxidation on Palladium in Acidic Solutions by On-Line Mass Spectroscopy. *J. Electroanal. Chem. Interf. Electrochem.* **1988**, *255* (1), 155–162.
(76) Miyake, H.; Okada, T.; Samjeské, G.; Osawa, M. Formic Acid Electrooxidation on Pd in Acidic Solutions Studied by Surface-Enhanced Infrared Absorption Spectroscopy. *Phys. Chem. Chem. Phys.* **2008**, *10* (25), 3662–3669.
(77) Zhang, H.-X.; Wang, S.-H.; Jiang, K.; André, T.; Cai, W.-B. In Situ Spectroscopic Investigation of CO Accumulation and Poisoning on Pd Black Surfaces in Concentrated HCOOH. *J. Power Sources* **2012**, *199*, 165–169.
(78) Baldauf, M.; Kolb, D. M. Formic Acid Oxidation on Ultrathin Pd Films on Au(Hkl) and Pt(Hkl) Electrodes. *J. Phys. Chem.* **1996**, *100* (27), 11375–11381.
(79) Hoyer, R.; Kibler, L. A.; Kolb, D. M. The Initial Stages of Palladium Deposition onto Pt(1 1 1). *Electrochim. Acta* **2003**, *49* (1), 63–72.
(80) Álvarez, B.; Climent, V.; Rodes, A.; M. Feliu, J. Potential of Zero Total Charge of Palladium Modified Pt(111) Electrodes in Perchloric Acid Solutions. *Phys. Chem. Chem. Phys.* **2001**, *3* (16), 3269–3276.
(81) Souza-Garcia, J.; Berná, A.; Ticianelli, E. A.; Climent, V.; Feliu, J. M. Electrochemical Properties of Palladium Adlayers on Pt(110) Substrates. *J. Electroanal. Chem.* **2011**, *660* (2), 276–284.

(82) Marković, N. M.; Lucas, C. A.; Climent, V.; Stamenković, V.; Ross, P. N. Surface Electrochemistry on an Epitaxial Palladium Film on Pt(111): Surface Microstructure and Hydrogen Electrode Kinetics. *Surf. Sci.* **2000**, *465* (1), 103–114.
(83) Arenz, M.; Stamenkovic, V.; Schmidt, T. J.; Wandelt, K.; Ross, P. N.; Markovic, N. M. The Electro-Oxidation of Formic Acid on Pt–Pd Single Crystal Bimetallic Surfaces. *Phys. Chem. Chem. Phys.* **2003**, *5* (19), 4242–4251.
(84) Chen, X. Adsorption and Catalysis on Pt and Pd Monolayer-Modified Pt Single Crystal Electrodes, PhD thesis, Leiden University, 2019.
(85) Kortlever, R.; Balemans, C.; Kwon, Y.; Koper, M. T. M. Electrochemical CO2 Reduction to Formic Acid on a Pd-Based Formic Acid Oxidation Catalyst. *Catal. Today* **2015**, *244*, 58–62.
(86) Koper, M. T. M. Theory of Multiple Proton–Electron Transfer Reactions and Its Implications for Electrocatalysis. *Chem. Sci.* **2013**, *4* (7), 2710–2723.
(87) Chen, X.; Koper, M. T. M. Mass-Transport-Limited Oxidation of Formic Acid on a PdMLPt(100) Electrode in Perchloric Acid. *Electrochem. commun.* **2017**, *82*, 155–158.